Chemical Science

ROYAL SOCIETY OF CHEMISTRY

EDGE ARTICLE

View Article Online
View Journal | View Issue

Cite this: *Chem. Sci.*, 2025, **16**, 709

All publication charges for this article have been paid for by the Royal Society of Chemistry

Regio- and diastereoselective synthesis of cyclobutylated phenothiazines *via* [2 + 2] photocycloaddition: demonstrating wavelength-gated cycloreversion inside live cells†

Sanhati Sharangi, ‡ Barsha Chakraborty, ‡ Raushan Kumar Jha, Swarnadeep Mandal, Apurba Lal Koner * and Sangit Kumar *

Herein, we unveiled a regio- and diastereoselective synthesis of cyclobutylated phenothiazines, a unique class of structural congeners of phenothiazines *via* visible-light-irradiated intermolecular [2 + 2]-cycloaddition reaction, from readily available naphthoquinones, 2-aminothiophenols, and styrenes, either in a two-step or three-component coupling process. By varying substitutions in all three coupling partners, a library of cyclobutylated phenothiazines, including late-stage derivatization with five commercial drugs, has been realized with up to 97% isolated yield. In contrast to the reported pathways, the developed [2 + 2]-photocycloaddition seems to proceed *via* a 'photoinduced-electron-transfer' (PET) mechanism, which is well corroborated with the experimental observations, Rehm–Weller equation, and computation studies. Delightfully, a wavelength-gated reversibility of the [2 + 2]-photocycloaddition reaction has been accomplished on the synthesized cyclobutylated phenothiazines. By monitoring the rate of the cycloreversion reactions for different derivatives, a structure–activity relationship has also been achieved. Interestingly, this phenomenon was further replicated inside living cells, which leads to turn-on emission and is applied for photoresponsive cell imaging. This marks the first report of a light-triggered [2 + 2]-cycloreversion phenomenon occurring inside a live cell, leading to cell imaging. Moreover, the synthesized drug derivatives were utilized for synchronous cell imaging as well as drug delivery through the developed [2 + 2]-photocycloreversion process, which demonstrated the potential applicability of this class of molecules.

Received 18th November 2024
Accepted 4th December 2024

DOI: 10.1039/d4sc07817a

rsc.li/chemical-science

Introduction

Facile synthesis of strained carbocyclic motifs, especially cyclobutane scaffolds, has garnered substantial interest in the past few decades for their use as valuable intermediate and molecular building blocks for synthesizing various natural products and pharmaceuticals.[1] Cyclobutanes, being the second most strained monocyclic alkanes in terms of total strain and strain per carbon atom,[2] can undergo facile ring expansion or fragmentation, producing the desired or active molecular structure. On the other hand, phenothiazines are very well known to be a valuable core in several commercially available drugs, *e.g.*, chlorpromazine, fluphenazine, methylene blue, *etc.* (Fig. 1a).[3] Since the pioneering discovery of phenothiazine in 1883 by Bernthsen, numerous derivatives of it have been synthesized to date and widely acknowledged for their remarkable bioactivity as well as extensive applications.[4] Phenothiazine drugs not only have revolutionized the realm of psychiatric medicines[5] but also exhibit significant contributions as antihistamines and antiemetics.[6] Due to this, the WHO has enlisted three phenothiazine drugs as essential medicines.[7]

In recent years, photocatalysis has increasingly become a valuable and potent technique for constructing diverse molecular assemblies that were previously challenging using conventional methods.[8] The greener, environmentally benign, and milder approach of this method facilitates the rapid construction of intricate molecular frameworks with reduced side products, thereby enhancing atom and step economy. In this context, various research groups across the world are utilizing photo-irradiated strategies for carbon–carbon,[9] and carbon–heteroatom[10] bond formation to access valuable molecules. Recently, the trend for monitoring a light-induced chemical reaction at the cellular level has gained significant

Department of Chemistry, Indian Institute of Science Education and Research (IISER) Bhopal, Academic Building – 2, Bhopal By-pass Road, Bhauri, Bhopal-462066, India. E-mail: akoner@iiserb.ac.in; sangitkumar@iiserb.ac.in

† Electronic supplementary information (ESI) available: Synthetic procedures, spectroscopic data, theoretical analysis and crystallographic information. CCDC 2332714 (**2a**), 2332712 (**2o**), 2403401 (**2x**), 2403402 (**2y**), 2332711 (**2ad**), 2403403 (**2af**), 2332713 (**2ak**), and 2403404 (**2al**). For ESI and crystallographic data in CIF or other electronic format see DOI: https://doi.org/10.1039/d4sc07817a

‡ Both contributed equally.

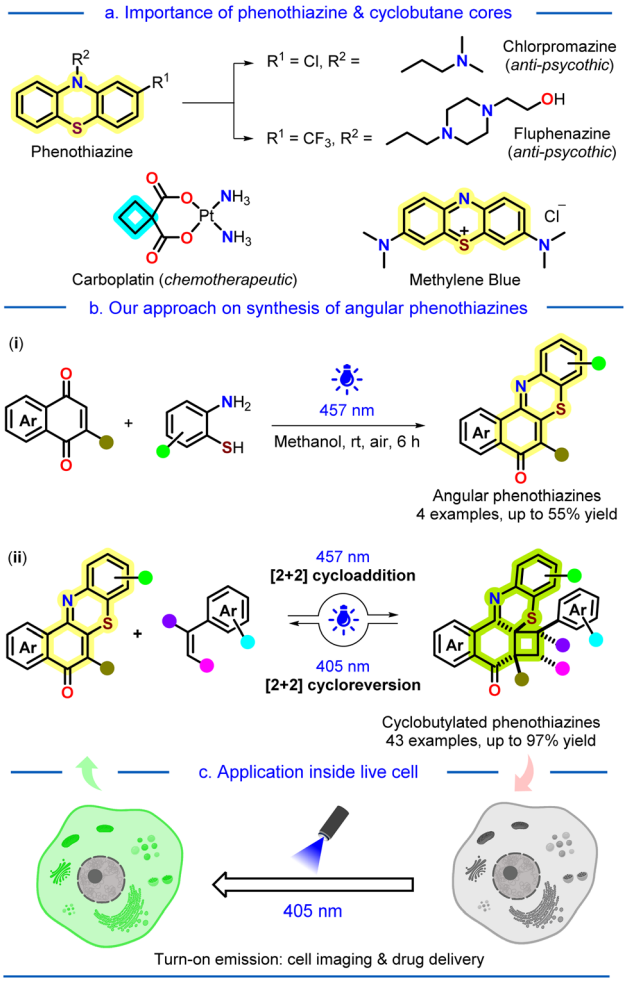

Fig. 1 (a) Importance of phenothiazine and cyclobutane cores; (b) our approach for synthesizing cyclobutylated phenothiazines *via* the light-irradiated pathway; (c) wavelength-gated [2 + 2] cycloreversion of the synthesized cyclobutylated phenothiazines inside live cells, utilized for cell imaging and drug delivery.

attention as this provides an appropriate insight into drug delivery and the mode of action of molecules for biological applications.[11] In this context, the cellular localization of a light-mediated chemical phenomenon is an attractive approach to manipulate and study subcellular events with high spatiotemporal resolution.

Our group is actively engaged in the development of organochalcogen (chalcogens = S, Se, and Te) chemistry, mainly accessing newer methodologies, preparing novel molecular architectures, and exploring their catalytic applications.[12]

In the last few years, we also have embarked on the light-driven construction of biologically relevant value-added molecules,[13] where very recently C–H-acylation, -amination, and -alkylation of naphthoquinones have been achieved by utilizing alcohols,[13c] amines,[13d] and even alkanes.[13e]

In this regard, we hypothesized whether we could make a unique conjuncture between the two structurally valuable cores: sulfur-heterocycle phenothiazine and cyclobutane, *via* a mild and sustainable light-driven protocol. The aim behind this hypothesis was to utilize this unique conjuncture for further cellular applications, as our laboratory is focused on synthesizing various small molecule fluorophores and utilizing them as markers for the bio-imaging of live cells.[14] Although phenothiazines are widely explored, their structural congener angular phenothiazines are underexplored despite their reported bioactivity.[15]

To our delight, at first, we successfully synthesized the angular phenothiazine **1** utilizing a visible-light-irradiated method by oxidative dehydrogenative coupling of C–H and S–H bonds of 1,4-quinones and aminothiophenols using aerial oxygen as an oxidant (Fig. 1b, eqn (i)). Finally, the synthesized angular phenothiazines **1**, upon light irradiated [2 + 2]-cycloaddition with styrenes, provided the desired cyclobutylated phenothiazines **2** (Fig. 1b, eqn (ii)) with excellent regio- & diastereoselectivity. A 'photoinduced electron transfer' (PET) mechanism has been proposed for the cycloaddition reaction, which is well corroborated with experimental observations as well as Density Functional Theory (DFT) studies. Later, we established a wavelength-gated reversibility in the synthesized cyclobutylated phenothiazines based on the subsequent photophysical studies and HPLC analysis. Further, this wavelength-gated photocycloreversion phenomenon was utilized for turn-on emission-mediated photoresponsive cell imaging and drug delivery for the first time (Fig. 1c).

Results and discussion

Initially, we sought to synthesize the angular phenothiazine **1a** through a conventional heating method using 1,4-naphthoquinone and 2-aminothiophenol *via* dehydrogenative oxidative coupling. We conducted the reactions using oxidants, namely, $Cu(OAc)_2$ and atmospheric oxygen, in the presence of solvents like DMSO and DMF. However, the desired transformation could not be achieved even by using conventional coupling between 2-bromo-1,4-naphthoquinone and 2-aminothiophenol. Next, by recognizing the exceptional reactivity of quinones under light-irradiated conditions,[13c–e,16] we sought to utilize the same in our quest to realize the angular phenothiazine **1a**.

Gratifyingly, under blue-light-irradiation (λ_{max} = 457 nm), the reaction of 1,4-naphthoquinone and 2-aminothiophenol yielded the angular phenothiazine **1a** in 40% yield in acetone under the aerial atmosphere.

Better yields (51 and 55%) of **1a** were realized in acetonitrile and methanol, keeping the light source unaltered (Scheme 1a, eqn (i)). 2-Amino-4-(trifluoromethyl)benzenethiol was also reacted smoothly with 1,4-naphthoquinone to enable trifluoromethyl-substituted angular phenothiazine **1ac** (see ESI, Page S6†). The coupling of 1,4-anthraquinone with 2-aminothiophenol occurred sluggishly to afford the respective angular phenothiazine **1ad** and was used further without any characterization (see ESI, Page S7†). The α,β-unsaturated double bond was tri-substituted in both **1ac** and **1ad**. To achieve a tetra-substituted derivative, 2-methylnaphthalene-1,4-dione was coupled with 2-aminobenzenethiol to afford **1ae** (see ESI, Page S7†).

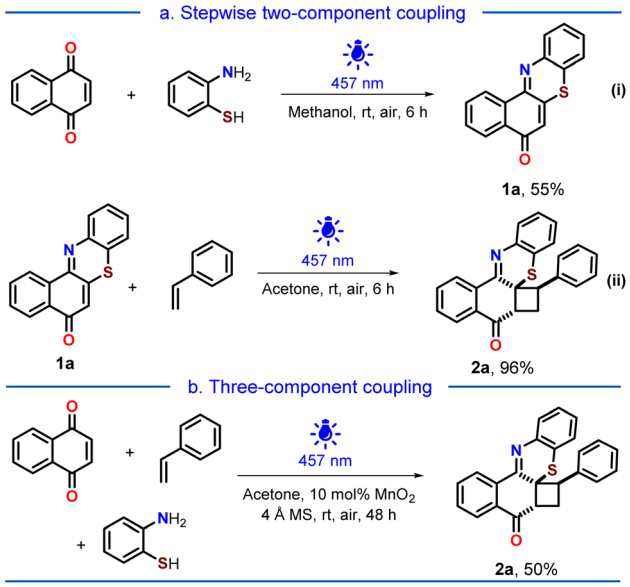

Scheme 1 Synthesis of the cyclobutylated phenothiazine **2a**: (a) stepwise two-component coupling (eqn (i) and (ii)); (b) three-component coupling.

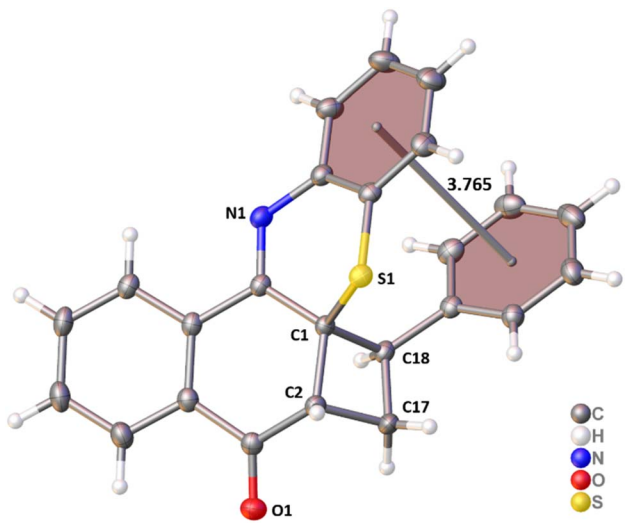

Fig. 2 Single crystal X-ray structure of cyclobutylated phenothiazine **2a** (CCDC no. 2332714).

The intermolecular [2 + 2] photocycloaddition between **1a** and styrene yielded the desired cyclobutylated phenothiazine **2a** in 96% isolated yield (Scheme 1a, eqn (ii)). Observing similar light-irradiated conditions for both steps, we were curious whether the cyclobutylated phenothiazine **2a** could be achieved *via* a three-component coupling. Realizing that an oxidative dehydrogenative coupling was occurring between 1,4-naphthoquinone and 2-aminothiophenol in the first step, we perceived that some reactive oxygen species might be generated in the reaction mixture as side products, which might impede the second step. Therefore, to facilitate the second step, we planned to quench the *in situ* generated species by introducing a catalytic amount of MnO_2 along with molecular sieves. Pleasingly, the desired cycloadduct **2a** was obtained in 50% yield from a three-component coupling process (Scheme 1b).

The regiochemistry and spatial arrangement of **2a** were assigned by its single crystal XRD analysis (Fig. 2), which revealed that a strong intramolecular π–π stacking interaction (3.765 Å) is present between the phenyl rings of styrene and benzothiazine. This intramolecular π–π stacking seems to be responsible for the excellent regio- and diastereoselectivity of the cycloadducts.

Substrate scopes

Next, we proceeded to the substrate scope variations (Scheme 2). To our delight, *o*-, *m*- and *p*-halogenated, alkylated, alkoxylated, arylated, and disubstituted styrenes underwent the [2 + 2]-photocycloaddition reaction very smoothly to afford the corresponding cyclobutylated phenothiazines **2a–2v** with excellent yields (82–97%). The 97% isolated yield of the cyclobutylated phenothiazine **2a** on gram-scale synthesis demonstrated the practical applicability of the developed protocol. The α- and *trans*-β-methylated styrenes provided moderate yields of **2w** and **2x**, probably due to increased steric crowding around the reactive double bond (54% and 58%). A 30% yield of the desired cycloadduct **2y** was obtained with *trans*-stilbene, while *cis*-stilbene led to only a trace amount of product **2z**. The electron-deficient 2- and 4-vinyl pyridines also exhibited only traces of their respective products **2aa** and **2ab**. Noteworthily, styrenes with electron-withdrawing substituents were unreactive toward the photocycloaddition reaction. Next, we varied the angular phenothiazine counterpart by taking trifluoromethyl-substituted angular phenothiazine **1ac** and 1,4-anthraquinone coupled angular phenothiazine **1ad** (Scheme 2b and c). Both of them reacted smoothly with styrene to afford the corresponding cyclobutylated phenothiazines **2ac** and **2ad** in 90% and 69% yields, respectively.

Thereafter, we proceed to investigate the scope of the developed [2 + 2] photocycloaddition reaction with tri- and tetrasubstituted double bond-containing precursors (Scheme 2d). When the tetrasubstituted phenothiazine **1ae** was reacted with styrene, it produced the corresponding cycloadduct **2ae** only in low yield (20%), presumably due to increased steric hindrance around the double bonds. We then explored the tri- and tetrasubstituted double bond containing styrenes in the photocycloaddition reaction. (Cyclopropylidenemethyl)benzene and 2-methyl-1*H*-indene provided the corresponding cycloadducts **2af** and **2ag** with moderate (50%) and low (15%) yields, respectively. However, trisubstituted styrenes with increased steric crowding around the double bond provided only traces of the corresponding products **2ah**, **2ai**, and **2aj**. The tetrasubstituted styrenes did not participate in the cycloaddition reaction at all. Alleviation of ring strain in the cyclopropyl ring upon [2 + 2] photocycloaddition in the case of **2af** might facilitate the reaction to provide comparatively better yield (50% *vs.* 20%-trace).

Moving forward, we proceed with the post-synthetic modification of our synthesized cyclobutylated phenothiazine **2a**

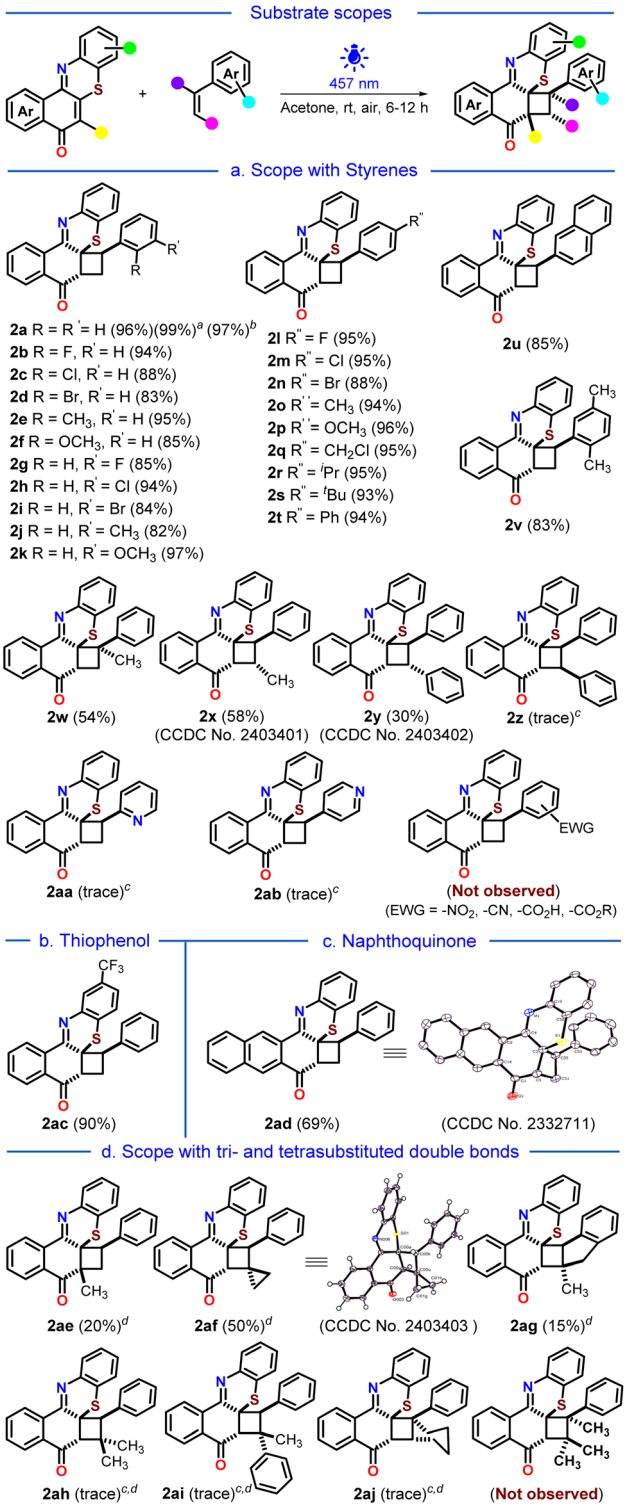

Scheme 2 Substrate scopes for the cycloaddition reaction [angular phenothiazine (1.0 equiv., 200 mg), styrene (3 equiv.), acetone (3 mL), 6 h]. [a]NMR yield, [b]gram scale synthesis [**1a** (1.0 g, 3.8 mmol), **2a** (1.3 mL, 11.4 mmol), acetone (10 mL), 6 h], [c]traces of the product were characterized by mass spectrometry, [d]reaction time 12 h.

(Scheme 3a). Upon reduction with $NaBH_4$, **2a** gets reduced to phenothiazin-8-ol **2ak**, which upon oxidation with *m*-CPBA results in the sulfoxide **2al** with good yields. Lastly, we pondered upon the possibility of combining the cyclobutylated phenothiazine **2a** with commercially available drug molecules (Scheme 3b). By following the reported procedures,[17] 4-chloromethyl styrene was coupled with five commercial drugs, namely, ibuprofen, flurbiprofen, gemfibrozil, clofibric acid, and fenbufen, to afford the corresponding drug-coupled styrenes.

To our delight, these drug-coupled styrenes reacted smoothly with the synthesized angular phenothiazine **1a** under the developed [2 + 2] photocycloaddition reaction conditions, providing the late-stage functionalization of cyclobutylated phenothiazine (**2am–2aq**) in moderate to good (50–72%) yields.

Control experiments for mechanistic understanding

After synthesizing a library of cyclobutylated phenothiazines, we turned our focus on gaining insights into the mechanism of the reaction by performing some control experiments (Scheme 4). To understand whether the reaction is proceeding *via* a concerted pathway or *via* a stepwise mechanism, we have performed radical trapping/quenching experiments. In the presence of the radical trapper TEMPO, not only was the yield of the desired product decreased, but three TEMPO adducts were also realized through the mass spectrometry analysis (Scheme 4a). Also, radical scavenger TBHP led to a decrement in the yield to 19% of the product (Scheme 4b). These experiments indicated that our photocycloaddition is proceeding *via* a stepwise pathway involving radical intermediates. Next, we performed the photocycloaddition in the presence of triplet state quenchers 9,10-phenanthrenequinone and ferrocene having triplet energies >60 kcal mol^{-1} (styrene has a triplet energy of ~60 kcal mol^{-1}), which lowered the yield of the cyclobutylated phenothiazine to 22% and 15%, respectively, indicated that the reaction might proceeds *via* a triplet excited state (Scheme 4c).

PET process verified using the Rehm–Weller equation

For the Rehm–Weller equation, the excited state redox potential of **1a** and ground state oxidation potential of styrene were obtained from cyclic voltammetry, absorption, and emission studies (see ESI, Pages S38 and S39†). The more positive, excited-state redox potential $E_{1/2}^{*\mathrm{Red}}(A)_{1/2}^{*\mathrm{Red}}$ value of angular phenothiazine **1a** (+1.765 V) in comparison to the one-electron oxidation potential value of styrene [$E_{1/2}^{\mathrm{Ox}}(D) = +1.1$ V] strongly suggested that angular phenothiazine **1a**, in its excited state, is capable of oxidizing the styrene. Further, the corresponding negative ΔG_{ET} value (−64.16 kJ mol^{-1}) strongly suggested the feasibility of a photoinduced electron transfer (PET) process.

DFT computation

To gain further insight into the plausible mechanism of the [2 + 2] photocycloaddition, we have studied the molecular orbitals of excited state phenothiazine **I** (see ESI, Fig. S12 and Page S51†) and styrene (see ESI, Fig. S11 and Page S51†). The calculated energy difference between the SOMO of excited state phenothiazine **I** and the HOMO of styrene is +6.11 kcal mol^{-1}. This indicated a feasible condition for electron transfer from styrene to excited state phenothiazine **I** under the blue-LED irradiation condition.

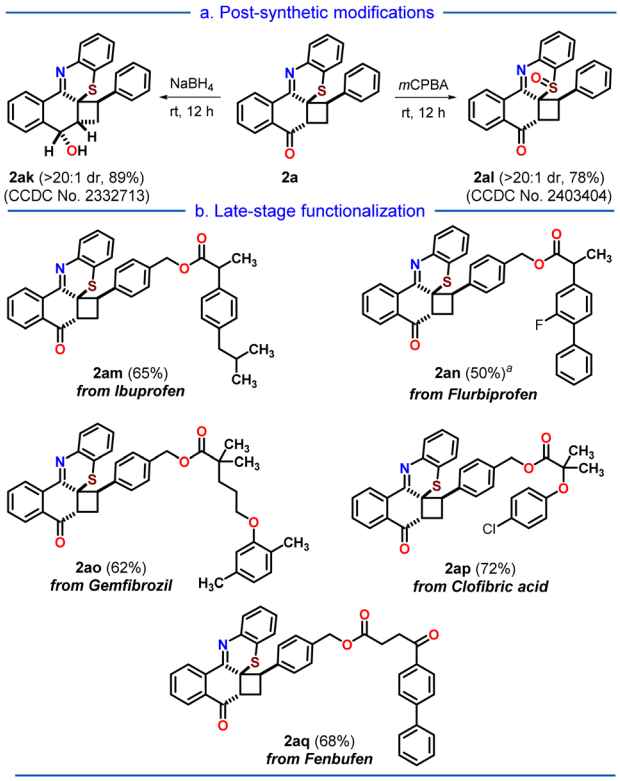

Scheme 3 (a) Post-synthetic modifications, and (b) late-stage drug derivatization of the cycloadduct **2a**; [a]Na_2EosinY (10 mol%) was added.

Photophysical investigations

Next, we turned our attention toward the photophysical investigations of synthesized molecules (see ESI, Fig. S5 and Page S31†). The synthesized angular phenothiazine **1a** exhibited distinct absorption at 470, 364, and 310 nm. However, the cyclobutylated phenothiazine **2a** provides a featureless broad absorption spectrum ranging from almost 322 nm to 455 nm with an absorbance maximum at 348 nm. Compared to the initial precursor of phenothiazines, namely, 1,4-naphthoquinone (λ_{max} = 330 nm), the absorption maxima of both the angular phenothiazine **1a** and cyclobutylated phenothiazine **2a** were red-shifted; where, in the case of **1a**, the red-shift is more prominent. Moreover, the angular phenothiazine **1a** shows significant emissive properties in comparison to 1,4-naphthoquinone and cyclobutylated phenothiazine **2a**.

Kinetic experiment of the [2 + 2] photocycloaddition reaction

To understand the kinetics of the photocycloaddition reaction, the blue light irradiated (λ_{max} = 457 nm) reaction mixture of angular phenothiazine **1a** and styrene was studied by UV-visible spectroscopy at different time intervals (Fig. 3). The absorption spectrum of the reaction mixture suggests that the angular phenothiazine **1a** and styrene precursors were nearly consumed after 360 minutes, as the maximum absorption at 470 nm corresponding to precursor **1a** gets saturated (Fig. 3a and b). This indicated that the reaction was completed within 360 minutes. A similar trend was also observed in emission spectra (see ESI, Fig. S8 and Page S35†).

Next, the rate of the [2 + 2] cycloaddition reaction was monitored by the UV-visible absorption, which indicated that the rate is linearly dependent on the concentration of angular phenothiazine **1a** and styrene. It follows first-order kinetics with respect to both the reactants individually with a rate constant of $(6.6 \pm 0.4) \times 10^{-3}$ min^{-1} (Fig. 3c). Further, the reaction rate was calculated from the respective rate constants for the initial 240 minutes of the reaction using the first-order rate law (see ESI, Pages S32 and S33†). The reaction rate for [2 + 2] cycloaddition was observed as 0.26 μM min^{-1} for the initial 240 minutes of the reaction.

Further, we have also investigated the dependency of the photocycloaddition reaction rate on the incident light intensity. For that, we conducted the reaction between angular phenothiazine **1a** and styrene under optimized reaction conditions, at

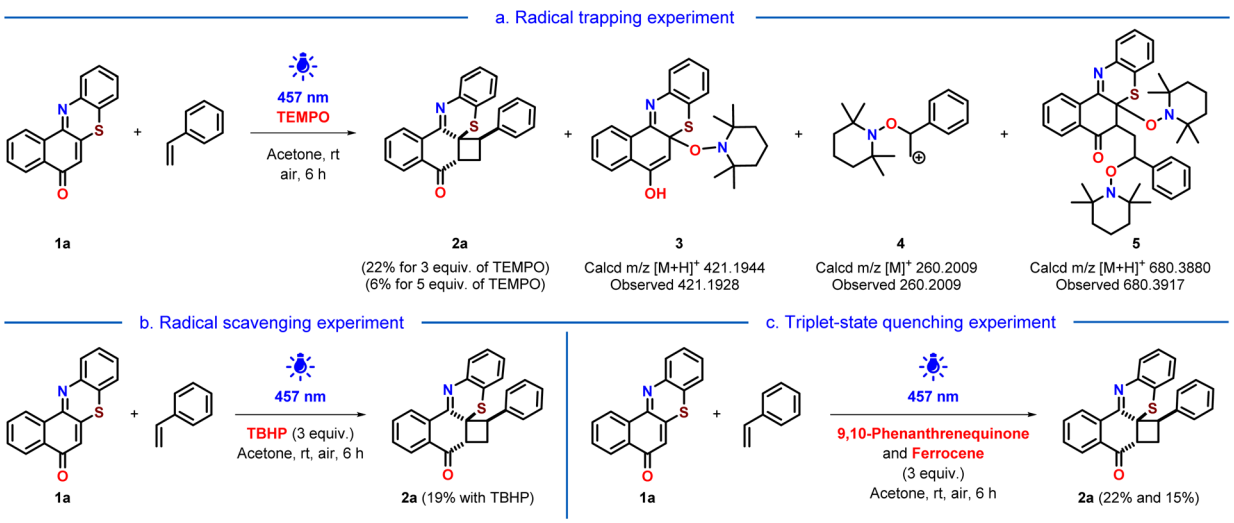

Scheme 4 Control experiments in the presence of (a) TEMPO, (b) TBHP, and (c) 9, 10-phenanthrenequinone and ferrocene.

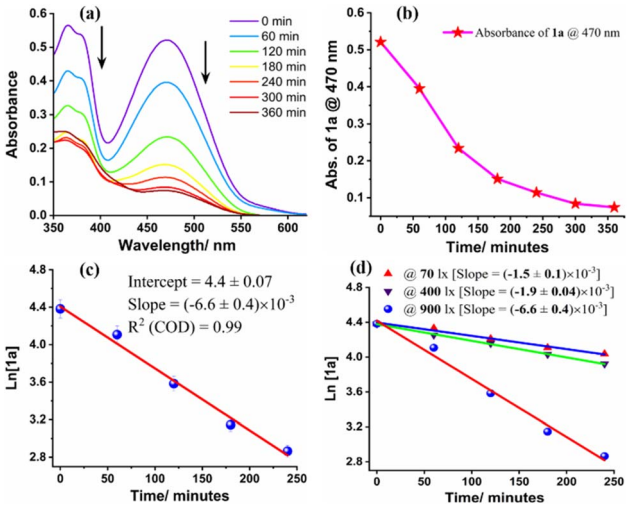

Fig. 3 Kinetic monitoring of the [2 + 2] cycloaddition reaction between angular phenothiazine **1a** and styrene: (a) time-dependent absorption spectra of the [2 + 2] photocycloaddition at 900 lx; (b) change in the absorbance at 470 nm of angular phenothiazine **1a** with respect to time; (c) plot of Ln[**1a**] with respect to time for determining the rate of reaction at 900 lx; (d) rate of the [2 + 2] cycloaddition reaction at different incident light intensities (lx). These studies were performed at 80 μM concentration in acetonitrile.

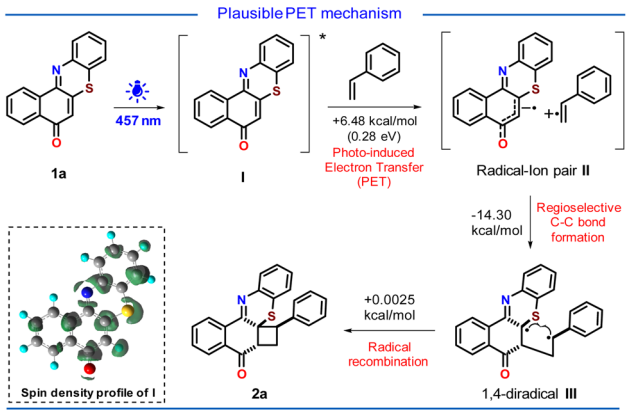

Scheme 5 Plausible reaction mechanism of the [2 + 2] photocycloaddition. The calculated relative Gibb's free energy of the reaction (Δ*G*° in kcal mol^{-1}) was obtained at a DFT-B3LYP/6-311+G(d,p)/CPCM(acetone) level of theory.

variable light intensities. The reactions were carried out up to saturation and the rate of each reaction was monitored up to 240 minutes (Fig. 3d).

At the optimal light intensity of 900 lx, the reaction rate was at its maximum (0.26 μM min^{-1}), with a rate constant of (6.6 ± 0.4) × 10^{-3} min^{-1} (see ESI, Page S33 and S34†). As the incident photon concentration decreased, the reaction rate also gradually declined. At 400 lx, the rate was 0.12 μM min^{-1} with a rate constant of (1.9 ± 0.04) × 10^{-3} min^{-1}, and at 70 lx, the rate was 0.097 μM min^{-1} with a rate constant of (1.5 ± 0.1) × 10^{-3} min^{-1}. These results are suggestive of the dependency of rate law on the intensity of incident light.

Proposed mechanism

Based on the above experimental observations and DFT computation (see ESI, Pages S40–S60†), we proposed a PET mechanism for the cycloaddition reaction (Scheme 5). Upon light irradiation, phenothiazine **1a** gets excited to produce the excited state phenothiazine **I**. The high oxidizing nature of the excited state phenothiazine **I** could facilitate the single electron transfer from styrene to the oxidizing excited state phenothiazine **I** to afford the radical–ion pair **II**. The electron transfer from styrene to the excited state phenothiazine moiety seems to be endergonic by 6.48 kcal mol^{-1} (0.28 eV). This is reasonably a feasible condition for photo-induced electron transfer. In the close proximity of the radical–ion pair **II**, the π–π stacking plays its role and helps in the regioselective formation of a C–C bond generating the 1,4-diradical **III**. This step is exergonic by −14.30 kcal mol^{-1} which indicates the feasibility of this path. Finally, the prompt radical recombination in **III** resulted in the desired cycloadduct **2a** with excellent regio and diastereoselectivity.

It is worth mentioning that the lower yield of the product in nonpolar solvents (see ESI, Table 1,† entry 4), traces of product formation with electron-deficient styrenes (**2aa** & **2ab**), and the nonreactivity of styrenes with electron-withdrawing substituents support this PET process.

From both the SOMOs of radical ion pair **II**, it can be seen that one of the electrons is lying on the phenothiazine backbone and the other electron is lying on the styrene backbone (Fig. 4). Also from the electron density plot, we have observed that most of the electron density is lying over the phenothiazine moiety (see ESI, Fig. S13 and Page S52†).

Here, it is worth noticing that the proposed PET process is in contrast to the literature precedences, where the [2 + 2] photocycloaddition between an enone and olefin is documented to proceed *via* an 'energy transfer' (EnT) process between an excited triplet-state enone and a ground-state olefin.[18]

Wavelength-gated [2 + 2] photocycloreversion of cyclobutylated phenothiazines

During these experiments, a color change was observed in cyclobutylated phenothiazine **2a** upon exposure to light. Before exposure to any light irradiation, the colorless solution of **2a** provides only a featureless broad absorption spectrum spanning from 322 nm to 455 nm (Fig. 5A, and ESI Fig. S5 and Page

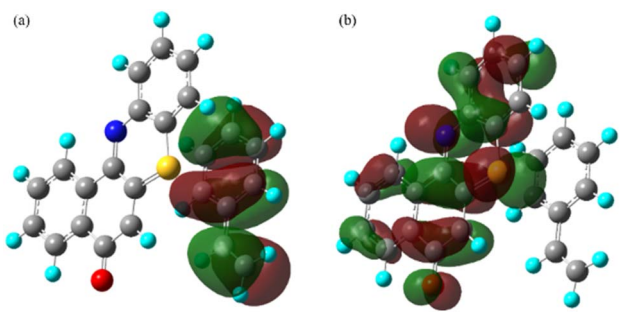

Fig. 4 (a) SOMO and (b) SOMO+1, pictures of radical–ion pair II.

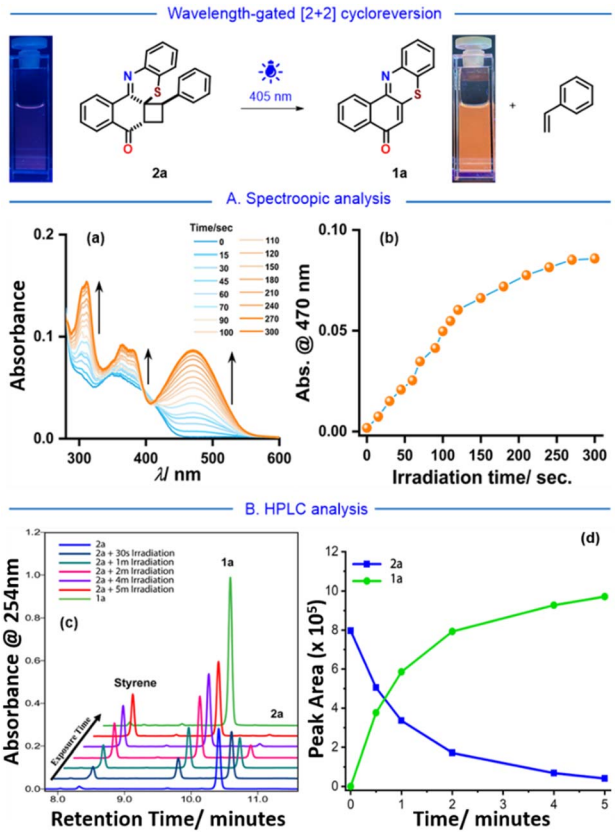

Fig. 5 Wavelength-gated [2 + 2] cycloreversion of cyclobutylated phenothiazine **2a** (10 μM in acetonitrile) upon irradiation with a 405 nm external laser source. (A) Spectroscopic analysis: (a) time-dependent UV-vis absorption spectra of **2a**; and (b) corresponding OD values at various time intervals. (B) HPLC analysis: (c) time-dependent HPLC analysis; and (d) concentration of **2a** and **1a** in the reaction mixture at various time intervals.

S31†). However, upon being subjected to an external laser source of 405 nm, the absorbance value of **2a** gradually increases beyond 455 nm and reveals well-defined vibronic features (λ_{max} = 470 nm). After 5 minutes of irradiation, the spectra became saturated, and the final spectrum perfectly mirrored the absorption spectrum of angular phenothiazine **1a**. This reshaping of absorption spectra indicated that upon light exposure, the cyclobutylated phenothiazine **2a** might be converting back to the angular phenothiazine **1a** *via* the [2 + 2] photocycloreversion process. Also, irradiation on different concentrations of cyclobutylated phenothiazine **2a** resulted in the complete conversion into angular phenothiazine **1a**, which indicated that the [2 + 2] photocycloreversion phenomenon is concentration-independent (Fig. S26 and Page S69, ESI†).

To further authenticate this phenomenon, a high-performance liquid chromatography (HPLC) experiment was conducted at various time intervals (Fig. 5B). Initially, a solution of cyclobutylated phenothiazine **2a** was examined to establish the peak retention time prior to any light exposure, revealing an isolated peak at 10.4 min. Exposure to the external laser source (405 nm) gave rise to two new peaks that precisely aligned with angular phenothiazine **1a** (9.8 min) and styrene (8.2 min). After 5 minutes of light exposure, the intensified peaks of **1a** and styrene, whereas the reduced peak of **2a** nearly to the baseline, indicated the spectrum saturation (see ESI, Fig. S21, Pages S60 and S61†). Eventually, this HPLC study authenticated that the [2 + 2] photocycloreversion of the synthesized cyclobutylated phenothiazine **2a** precisely produced back its precursors, namely, angular phenothiazine **1a** and styrene, without formation of any side product.

Cell imaging and drug delivery by the developed wavelength-gated [2 + 2] photocycloreversion

Having these experimental results, we were intrigued by the prospect of replicating the developed light-triggered [2 + 2] cycloreversion phenomenon within live cells, aiming for cell imaging. To ascertain the feasibility of this process within biological systems, a similar light-triggered [2 + 2] cycloreversion reaction was performed in PBS (Fig. S27 and Page S69, ESI†).

To explore cell viability, we examined the cytotoxicity of both the synthesized angular phenothiazine **1a** and cyclobutylated phenothiazine **2a** probes using the MTT assay in live HeLa cells (Fig. 6). The results showed that more than 80% of the cells remained viable at 5 μM concentration of both probes, affirming their suitability for cell imaging. The green fluorescence emitting from all over the cells upon treatment with angular phenothiazine **1a** indicated a good distribution of the probe throughout the cytoplasm. In contrast, the cyclobutylated phenothiazine **2a** probe did not exhibit any significant fluorescence in the green channel under normal conditions.

Next, to conduct the [2 + 2] cycloreversion experiment, HeLa cells were pre-treated with cyclobutylated phenothiazine **2a** for 15 minutes, and subsequent images were acquired. As expected, the FITC channel does not show any fluorescence despite healthy cells being visualized from the DIC images (Fig. 7a). Surprisingly when cells in the same field of view (FOV) were irradiated for 30 seconds with an external laser source (405 nm), an intense green fluorescence was observed from all over the cells (Fig. 7b). The intensity became more prominent after 1 minute of irradiation (Fig. 7c). The merged images displayed how the cells glowed up after light irradiation. Therefore, considering all the experimental outcomes, we postulated that within the cellular environment as well, upon light-irradiation,

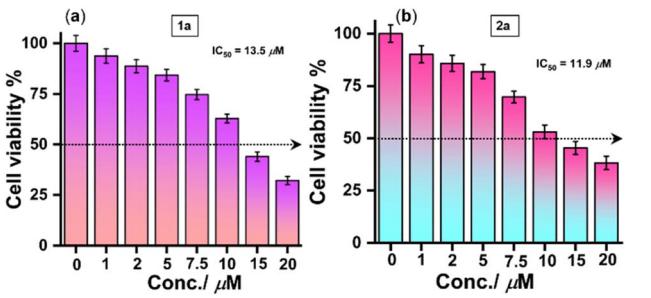

Fig. 6 Cell viability assay in live HeLa cells for (a) angular phenothiazine **1a** and (b) cyclobutylated phenothiazine **2a** probes, respectively.

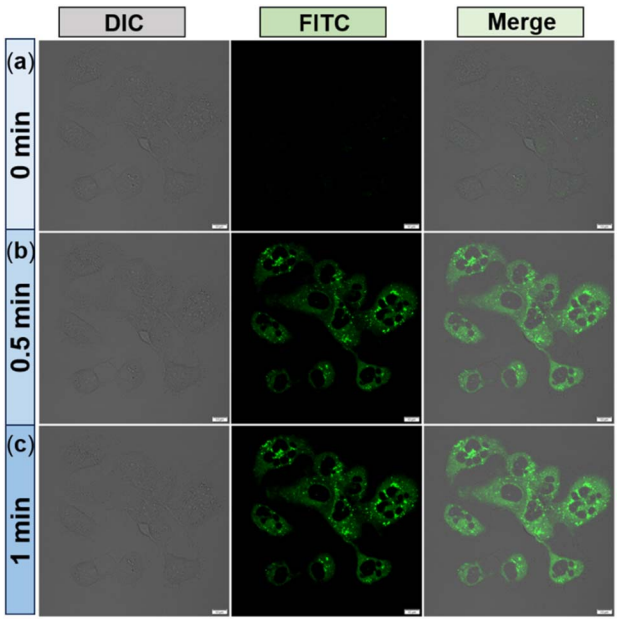

Fig. 7 Confocal laser scanning microscopy (CLSM) images of HeLa cells after treatment with 5 μM of cyclobutylated probe **2a** upon irradiation without (upper panel: (a)) and with (middle and lower panel: (b) and (c)) light. Scale bar = 10 μm.

the non-fluorescent cyclobutylated phenothiazine **2a** undergoes a [2 + 2] cycloreversion to generate fluorescent angular phenothiazine **1a**.

It is worth mentioning that, to the best of our knowledge, this presents the first report of a light-triggered [2 + 2] photocycloreversion reaction occurring inside a cell, resulting in a remarkable turn-on emission that leads to photoresponsive live cell imaging.

Further, the internalization pathway of the angular phenothiazine **1a** was investigated in order to understand how this probe stains the cytoplasm. As depicted in Fig. S29 (Page S70, ESI),† when HeLa cells were incubated at a low temperature, the fluorescence intensity coming from the cytoplasm was significantly reduced. This result suggests that the angular phenothiazine **1a** probe might be penetrating the cells through an energy-dependent pathway.

To gain deeper insight into a particular endocytosis pathway involved in the internalization of **1a**, several cellular uptake assays were carried out in the presence of various inhibitors such as chloroquine (CQ), chlorpromazine (CPZ), methyl-β-cyclodextrin (MβCD), amiloride hydrochloride (AMR) and cytochalasin-D (CyD). According to Fig. S29 and S30 (Pages S71, ESI),† there is no substantial alteration in the fluorescence intensity when cells were treated with CQ, CPZ, MβCD, AMR, and CyD compared to the control group. This suggested that the endocytosis pathway of the angular phenothiazine **1a** is independent of autophagic flux, clathrin, and lipid raft, as well as micropinocytosis and phagocytosis through actin polymerization. The corresponding fluorescence intensities were plotted to better represent the effect of cellular internalization at a low temperature and in the presence of different inhibitors (Fig. S30, ESI†). It is evident from Fig. S30† that cellular uptake is majorly affected when the cells were kept at 4 °C for incubation.

All these results implied that cellular uptake of the angular phenothiazine **1a** occurs through an energy-dependent pathway. Encouraged by these results, we next proceeded to investigate the structure–activity relationship of the synthesized cyclobutylated phenothiazines in terms of the rates of their cycloreversion reactions. Consequently, we have performed the [2 + 2] photocycloreversion reaction of the synthesized cycloadducts **2a–2af** using the external laser source of 405 nm and monitored the corresponding time-dependent UV-visible absorption data (for a detailed discussion see ESI, Page S62–S66†). When *ortho*-, *meta*- and *para*-substituted cyclobutylated phenothiazines were compared, a general trend was observed that the *ortho*-substituted ones **2b**, **2d**, **2e**, and **2f** were exhibiting the highest rates while the *meta*-substituted cycloadducts **2l**, **2n**, **2o**, and **2p** were the slowest. *Para*-substituted cycloadducts **2g**, **2i**, **2j**, and **2k** showed rates in between *ortho*- and *meta*-ones (see ESI, Page S63†). Further, when the rates of the photocycloreversion of all the synthesized cycloadducts were compared, it was found that among all the cyclobutylated phenothiazines, the *ortho*-methyl substituted cyclobutylated phenothiazine **2e** exhibited the highest rate (0.049 μM s^{-1}), whereas the *trans*-stilbene derived cycloadduct **2y** provided the slowest rate (0.016 μM s^{-1}). As can be seen from Fig. 8, the rate of cycloreversion of **2e** is three times higher in comparison to **2y**. Subsequently, we proceeded to explore the structure–activity relationship within live HeLa cells and observed that in the case of **2e**, no signal was detected from the cells prior to light irradiation (Fig. 9a). However, after 1 minute of irradiation, a significant enhancement in signal intensity was observed

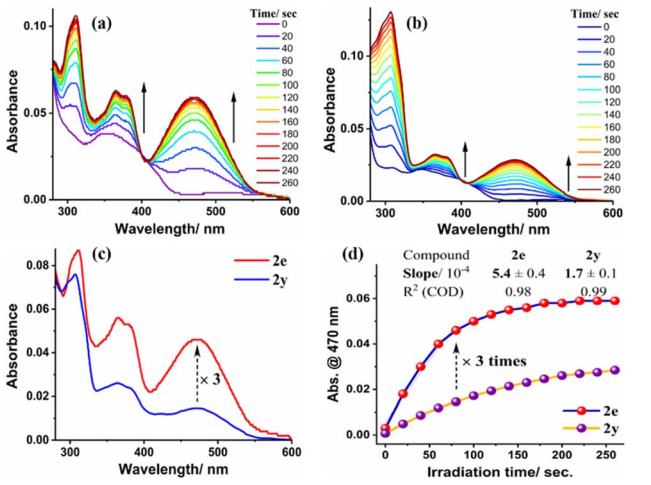

Fig. 8 (a) Time-dependent UV-vis absorption spectra of **2e** for photocycloreversion; (b) time-dependent UV-vis absorption spectra of **2y** for photocycloreversion; (c) comparison of the absorption spectra of **2e** and **2y** after 80 seconds of photoirradiation: **2e** exhibited three times higher absorbance than **2y**; (d) comparison of the rates of [2 + 2] photocycloreversion of **2e** and **2y** after 80 seconds of photoirradiation: rate of **2e** was three times higher than that of **2y**. These studies were performed at 5 μM concentration in acetonitrile.

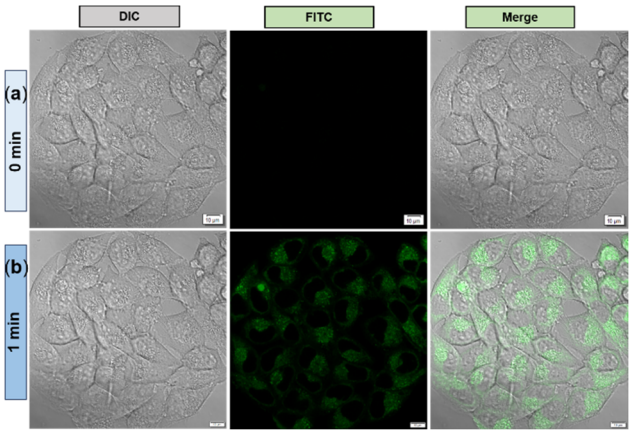

Fig. 9 Confocal laser scanning microscopy (CLSM) images of HeLa cells after treatment with 5 μM of probe **2e** upon without irradiation (upper panel (a)) and with irradiation (lower panel (b)).

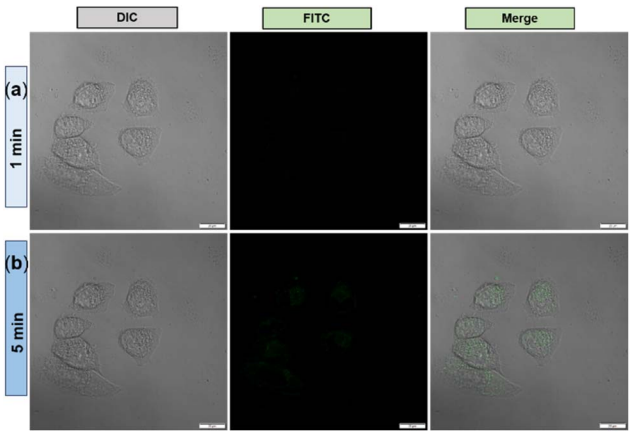

Fig. 10 Confocal laser scanning microscopy (CLSM) images of HeLa cells after treatment with 5 μM of probe **2y** upon 1 min irradiation (upper panel (a)) and 5 min irradiation (lower panel (b)).

throughout the cells, which was visible in the FITC channel (Fig. 9b). On the other hand, when the cells were treated with **2y** and subjected to photo-irradiation, no distinguishable signal was observed in the FITC channel after 1 minute of irradiation (Fig. 10a).

Even after 5 minutes of irradiation, only a very weak emission signal was detected in the FITC channel (Fig. 10b), suggesting that the stilbene-derived **2y** undergoes cycloreversion at a slower rate than *ortho*-methylated **2e** and it takes a longer time for cell imaging. Therefore, the cellular experimental observations were well corroborated with the corresponding spectroscopic evidence, demonstrating the structure–activity relationship.

Encouraged by this, we were curious to explore whether both cell imaging as well as drug delivery could be achieved, by replicating the photocycloreversion phenomenon with drug-coupled cyclobutylated phenothiazines (**2am–2aq**). Ibuprofen-coupled cyclobutylated phenothiazine **2am** was taken as the representative probe, and its UV-visible absorption spectra revealed that upon light irradiation, it undergoes similar [2 + 2] cycloreversion (see ESI, Fig. S31 and Page S71†). Gratifyingly, within the HeLa cell as well, the probe was enabled for light-triggered cell imaging (see ESI, Fig. S32 and Page S72†), indicating the release of the ibuprofen moiety inside the cell. The further impact of the released drug is currently under investigation.

Conclusions

In summary, a mild and sustainable visible light irradiated protocol has been introduced to develop a new series of distinctly regio- and diastereoselective cyclobutylated phenothiazines from readily available naphthoquinones, 2-aminothiophenols, and styrenes either *via* a two-step or a one-pot-three-component coupling pathway. The developed photocycloaddition between the synthesized angular phenothiazines and styrenes seems to proceed *via* a PET mechanism, based on the substrate scope observations, experimental findings, and computational studies. A wavelength-gated [2 + 2] photocycloreversion was realized and elucidated by spectroscopic and HPLC analyses. We could successfully replicate this photocycloreversion phenomenon inside live cells, which leads to turn-on emission and is utilized for photoresponsive live cell imaging. Utilizing the synthesized drug-coupled cyclobutylated phenothiazines, we have achieved photoresponsive synchronous cell imaging and drug delivery, which could be further extended to theranostic types of applications. Moreover, by monitoring the photocycloreversion rates of various derivatives, a structure–activity relationship was established and further explored within live HeLa cells. To the best of our knowledge, this presents the first instance of a [2 + 2] photocycloreversion reaction occurring inside a cell, resulting in photoresponsive live cell imaging and drug delivery. Therefore, the presented work not only demonstrates its potential for exploring further theranostic types of applications but also opens up new avenues for developing innovative bio-probes.

Data availability

Detailed synthetic procedures, reaction condition optimization, data characterization, controlled experiments, X-ray diffraction structural analyses, and geometries and energies of theoretically investigated structures have been provided in the ESI.†

Author contributions

SK and SS designed the project and wrote the manuscript. All the compounds have been synthesized and characterized by SS and SM. Kinetic studies, mechanistic investigations, photophysical studies, structure–activity relationship and related optical spectroscopy experiments were done by SS. RKJ carried out DFT computation. Cells and related optical spectroscopy experiments have been designed by ALK and BC and performed by BC. The cell biology and related spectroscopy part were written by BC and ALK.

Conflicts of interest

The authors declare no conflicts of interest.

Acknowledgements

SK acknowledges DST-SERB (CRG/2023/002473), New Delhi, and IISER Bhopal for financial support. SS acknowledges DST-INSPIRE (IF170996) for the fellowship. BC and RKJ acknowledge IISER Bhopal for the fellowship. Dr Debasish Manna (IISER Bhopal) and Mr Pritam Kumar Pain (IISER Bhopal) are sincerely acknowledged for the HPLC experiment. Dr Sachin Dev Verma (IISER Bhopal) is sincerely acknowledged for his guidance in the light intensity-dependent kinetics study. Dr Saravanan Raju is sincerely acknowledged for his help with single-crystal analysis. Miss Nisha is acknowledged for helping in synthesizing a few compounds. Mr Svastik Jaiswal is acknowledged for the CV experiments. ALK thanks IISERB for the funding and infrastructural support. We also acknowledge the confocal facility at IISER Bhopal.

Notes and references

1 (*a*) J. D. Winkler, C. M. Bowen and F. Liotta, *Chem. Rev.*, 1995, **95**, 2003–2020; (*b*) E. Lee-Ruff and G. Mladenova, *Chem. Rev.*, 2003, **103**, 1449–1483; (*c*) J. C. Namyslo and D. E. Kaufmann, *Chem. Rev.*, 2003, **103**, 1485–1537; (*d*) P. Raster, S. Weiss, G. Hilt and B. König, *Synthesis*, 2011, **6**, 905–908; (*e*) Y. Xu, M. L. Conner and M. K. Brown, *Angew. Chem., Int. Ed.*, 2015, **54**, 11918–11928; (*f*) S. K. Pagire, A. Hossain, L. Traub, S. Kerres and O. Reiser, *Chem. Commun.*, 2017, **53**, 12072–12075.

2 (*a*) N. L. Allinger, M. T. Tribble, M. A. Miller and D. H. Wertz, *J. Am. Chem. Soc.*, 1971, **93**, 1637–1648; (*b*) A. de Meijere, *Angew Chem. Int. Ed. Engl.*, 1979, **18**, 809–826; (*c*) Cyclobutane-Physical Properties and Theoretical Studies: K. B. Wiberg in *The Chemistry of Cyclobutanes*, Part 1, ed. Z. Rappoport and J. F. Liebman, Wiley, Chichester, 2005, pp. 1–15; (*d*) K. B. Wiberg, Z. Rappoport and J. F. Liebman, in *The Chemistry of Cyclobutanes*, John Wiley and Sons Inc, 2005.

3 Phenothiazines, DrugBank Online: **https://go.drugbank.com/categories/DBCAT000801**.

4 (*a*) A. Bernthsen, *Ber. Dtsch. Chem. Ges.*, 1883, **16**, 2896–2904; (*b*) K. Pluta, B. M. Młodawska and M. Jeleń, *Eur. J. Med. Chem.*, 2011, **46**, 3179–3189; In the treatment of prion diseases: (*c*) C. Korth, B. C. H. May, F. E. Cohen and S. B. Prusiner, *Proc. Natl. Acad. Sci. U. S. A.*, 2001, **98**, 9836; As antimalarial: (*d*) M. Kalkanidis, N. Klonis, L. Tilley and L. W. Deady, *Biochem. Pharmacol.*, 2002, **63**, 833; As antitubercular: (*e*) A. J. Warman, T. S. Rito, N. E. Fisher, D. M. Moss, N. G. Berry, P. M. O'Neill, S. A. Ward and G. A. Biagini, *J. Antimicrob. Chemother.*, 2013, **68**, 869; (*f*) D. Addla, A. Jallapally, D. Gurram, P. Yogeeswari, D. Sriram and S. Kantevari, *Bioorg. Med. Chem. Lett.*, 2014, **24**, 233; As cancer cell inhibitors: (*g*) X.-J. Dai, L.-J. Zhao, L.-H. Yang, T. Guo, L.-P. Xue, H.-M. Ren, Z.-L. Yin, X.-P. Xiong, Y. Zhou, S.-K. Ji, H.-M. Liu, H. -M. Liu, Y. Liu and Y.-C. Zheng, *J. Med. Chem.*, 2023, **66**, 3896–3916; As organic sensitizer: (*h*) H. Tian, X. Yang, R. Chen, Y. Pan, L. Li, A. Hagfeldt and L. Sun, *Chem. Commun.*, 2007, 3741–3743; (*i*) C.-J. Yang, Y. J. Chang, M. Watanabe, Y.-S. Hon and T. J. Chow, *J. Mater. Chem.*, 2012, **22**, 4040–4049; Antioxidants in lubricants and fuels in petroleum industries: (*j*) C. M. Rarner, H. Murphy and N. L. Smith, *Ind. Eng. Chem.*, 1950, **42**, 2479; As sensitizers for dye-sensitized solar cells: (*k*) A. F. Buene, E. E. Ose, A. G. Zakariassen, A. Hagfeldt and B. H. Hoff, *J. Mater. Chem. A*, 2019, **7**, 7581–7590; Miscellaneous: (*l*) R. Y. Lai, X. Kong, S. A. Jenekhe and A. J. Bard, *J. Am. Chem. Soc.*, 2003, **125**, 12631–12639; (*m*) D. Sun, S. V. Rosokha and J. Kochi, *J. Am. Chem. Soc.*, 2004, **126**, 1388–1401; (*n*) E. A. Weiss, M. J. Tauber, R. F. Kelley, M. J. Ahrens, M. A. Ratner and M. R. Wasielewski, *J. Am. Chem. Soc.*, 2005, **127**, 11842–11850; (*o*) H. W. Rhee, S. J. Choi, S. H. Yoo, Y. O. Jang, H. H. Park, R. M. Pinto, J. C. Cameselle, F. J. Sandoval, S. Roje, K. Han, D. S. Chung, J. Suh and J. I. Hong, *J. Am. Chem. Soc.*, 2009, **131**, 10107–10112.

5 (*a*) Phenothiazine antipsychotics, **https://www.drugs.com/drug-class/phenothiazine-antipsychotics.html**;; (*b*) How do phenothiazine antipsychotics work?, **https://www.rxlist.com/antipsychotics_phenothiazine/drug-class.htm**:.

6 (*a*) Phenothiazine antiemetics, **https://www.drugs.com/drug-class/phenothiazine-antiemetics.html**;; (*b*) Phenergan, **https://www.drugs.com/phenergan.html#side-effects**.

7 WHO Model List of Essential Medicines – 23rd list, 2023.

8 (*a*) M. D. Kärkäs, *ACS Catal.*, 2017, **7**, 4999–5022; (*b*) H. Yi, G. Zhang, H. Wang, Z. Huang, J. Wang, A. K. Singh and A. Lei, *Chem. Rev.*, 2017, **117**, 9016–9085; (*c*) Y. Sakakibara, E. Ito, T. Kawakami, S. Yamada, K. Murakami and K. Itami, *Chem. Lett.*, 2017, **46**, 1014–1016; (*d*) C. Song, X. Dong, Z. Wang, K. Liu, C.-W. Chiang and A. Lei, *Angew. Chem., Int. Ed.*, 2019, **58**, 12206–12210; (*e*) A. M. Nair, S. Kumar and C. M. R. Volla, *Adv. Synth. Catal.*, 2019, **361**, 4983–4988; (*f*) J. Kim, D. Kim and S. Chang, *J. Am. Chem. Soc.*, 2020, **142**, 19052–19057; (*g*) S. Wang, H. Wang and B. König, *J. Am. Chem. Soc.*, 2021, **143**, 15530–15537; (*h*) B. Maeda, G. Mori, Y. Sakakibara, A. Yagi, K. Murakami and K. Itami, *Asian J. Org. Chem.*, 2021, **10**, 1428–1431; (*i*) B. Maeda, Y. Sakakibara, K. Murakami and K. Itami, *Org. Lett.*, 2021, **23**, 5113–5117; (*j*) M. J. Genzink, J. B. Kidd, W. B. Swords and T. P. Yoon, *Chem. Rev.*, 2022, **122**, 1654–1716; (*k*) Y.-M. Tian, H. Wang, Ritu and B. König, *Chem. Sci.*, 2022, **13**, 241–246; (*l*) Z. Yang, D. Yang, J. Zhang, C. Tan, J. Li, S. Wang, H. Zhang, Z. Huang and A. Lei, *J. Am. Chem. Soc.*, 2022, **144**, 13895–13902; (*m*) R. Rahaman, A. M. Nair and C. M. R. Volla, *Chem.–Eur. J.*, 2022, **28**, e202201290; (*n*) W. Liu, Y. Ke, C. Liu and W. Kong, *Chem. Commun.*, 2022, **58**, 11937–11940; (*o*) S. K. Jana, M. Maiti, P. Dey and B. Maji, *Org. Lett.*, 2022, **24**, 1298–1302; (*p*) A. Ghosh, P. Pyne, S. Ghosh, D. Ghosh, S. Majumder and A. Hajra, *Green Chem.*, 2022, **24**, 3056–3080; (*q*) P. Bellotti,

H.-M. Huang, T. Faber and F. Glorius, *Chem. Rev.*, 2023, **123**, 4237–4352; (*r*) R. Kleinmans, S. Dutta, K. Ozols, H. Shao, F. Schäfer, R. E. Thielemann, H. T. Chan, C. G. Daniliuc, K. N. Houk and F. Glorius, *J. Am. Chem. Soc.*, 2023, **145**, 12324–12332; (*s*) P. Bellotti and F. Glorius, *J. Am. Chem. Soc.*, 2023, **145**, 20716–20732; (*t*) I. Halder, A. M. Nair and C. M. R. Volla, *Chem. Commun.*, 2023, **59**, 5862–5865; (*u*) S. Gupta, A. Kundu, S. Ghosh, A. Chakraborty and A. Hajra, *Green Chem.*, 2023, **25**, 8459–8493; (*v*) S. Ghosh, P. Pyne, A. Ghosh, S. Choudhury and A. Hajra, *Org. Biomol. Chem.*, 2023, **21**, 1591–1628; (*w*) N. S. Shlapakov, A. D. Kobelev, J. V. Burykina, A. Y. Kostyukovich, B. König and V. P. Ananikov, *Angew. Chem., Int. Ed.*, 2024, **63**, e202314208.

9 (*a*) W. Xie, S.-W. Park, H. Jung, D. Kim, M.-H. Baik and S. Chang, *J. Am. Chem. Soc.*, 2018, **140**, 9659–9668; (*b*) L. Niu, J. Liu, X.-A. Liang, S. Wang and A. Lei, *Nat. Commun.*, 2019, **10**, 467; (*c*) P. Rai, K. Maji and B. Maji, *Org. Lett.*, 2019, **21**, 3755–3759; (*d*) S. Xu, H. Chen, Z. Zhou and W. Kong, *Angew. Chem., Int. Ed.*, 2021, **60**, 7405–7411; (*e*) Z. Guan, X. Zhong, Y. Ye, X. Li, H. Cong, H. Yi, H. Zhang, Z. Huang and A. Lei, *Chem. Sci.*, 2022, **13**, 6316–6321; (*f*) W. Liu, C. Liu, M. Wang and W. Kong, *ACS Catal.*, 2022, **12**, 10207–10221; (*g*) K. Maji, P. R. Thorve, P. Rai and B. Maji, *Chem. Commun.*, 2022, **58**, 9516–9519; (*h*) P. Rai, K. Maji, S. K. Jana and B. Maji, *Chem. Sci.*, 2022, **13**, 12503–12510; (*i*) S. Laru, S. Bhattacharjee and A. Hajra, *Chem. Commun.*, 2022, **58**, 13604; (*j*) S. Xu, Y. Ping, W. Li, H. Guo, Y. Su, Z. Li, M. Wang and W. Kong, *J. Am. Chem. Soc.*, 2023, **145**, 5231–5241.

10 (*a*) S. Mukherjee, B. Maji, A. Tlahuext -Aca and F. Glorius, *J. Am. Chem. Soc.*, 2016, **138**, 16200–16203; (*b*) L. Niu, H. Yi, S. Wang, T. Liu, J. Liu and A. Lei, *Nat. Commun.*, 2017, **8**, 14226; (*c*) E. Ito, T. Fukushima, T. Kawakami, K. Murakami and K. Itami, *Chem*, 2017, **2**, 383–392; (*d*) I. Ghosh, J. Khamrai, A. Savateev, N. Shlapakov, M. Antonietti and B. König, *Science*, 2019, **365**, 360–366; (*e*) W. Lee, H. J. Jeon, H. Jung, D. Kim, S. Seo and S. Chang, *Chem*, 2021, **7**, 495–508; (*f*) S. Neogi, A. K. Ghosh, S. Mandal, D. Ghosh, S. Ghosh and A. Hajra, *Org. Lett.*, 2021, **23**, 6510–6514; (*g*) Y. Sakakibara, K. Itami and K. Murakami, *ChemRxiv*, 2022, preprint, DOI: **10.26434/chemrxiv-2022-drf9p**; (*h*) Z. Zhou, J. Kweon, H. Jung, D. Kim, S. Seo and S. Chang, *J. Am. Chem. Soc.*, 2022, **144**, 9161–9171; (*i*) W. Lee, D. Kim, S. Seo and S. Chang, *Angew. Chem., Int. Ed.*, 2022, **61**, e202202971; (*j*) A. Jati, K. Dey, M. Nurhuda, M. A. Addicoat, R. Banerjee and B. Maji, *J. Am. Chem. Soc.*, 2022, **144**, 7822–7833; (*k*) G. Tan, F. Paulus, A. Petti, M.-A. Wiethoff, A. Lauer, C. Daniliuc and F. Glorius, *Chem. Sci.*, 2023, **14**, 2447–2454; (*l*) H. Wang, H. Shao, A. Das, S. Dutta, H. T. Chan, C. Daniliuc, K. N. Houk and F. Glorius, *Science*, 2023, **381**, 75–81; (*m*) H. Wang, Z. Liu, A. Das, P. Bellotti, S. Megow, F. Temps, X. Qi and F. Glorius, *Nat. Synth.*, 2023, **2**, 1116–1126; (*n*) I. Ghosh, N. Shlapakov, T. A. Karl, J. Düker, M. Nikitin, J. V. Burykina, V. P. Ananikov and B. König, *Nature*, 2023, **619**, 87–93; (*o*) J. A. C. Delgado, Y.-M. Tian, M. Marcon, B. König and M. W. Paixão, *J. Am. Chem. Soc.*, 2023, **145**, 26452–26462; (*p*) S. Khan, A. M. Nair and C. M. R. Volla, *Org. Chem. Front.*, 2023, **10**, 157–162; (*q*) A. Jati, S. Dam, S. Kumar, K. Kumar and B. Maji, *Chem. Sci.*, 2023, **14**, 8624–8634; (*r*) A. K. Ghosh, S. Neogi, P. Ghosh and A. Hajra, *Adv. Synth. Catal.*, 2023, **365**, 2271–2278; (*s*) H. Keum, H. Ryoo, D. Kim and S. Chang, *J. Am. Chem. Soc.*, 2024, **146**, 1001–1008.

11 (*a*) D. H. M. Dam, J. H. Lee, P. N. Sisco, D. T. Co, M. Zhang, M. R. Wasielewski and T. W. Odom, *ACS Nano*, 2012, **6**, 3318–3326; (*b*) I. Roy, S. Bobbala, J. Zhou, M. T. Nguyen, S. K. M. Nalluri, Y. Wu, D. P. Ferris, E. A. Scott, M. R. Wasielewski and J. F. Stoddart, *J. Am. Chem. Soc.*, 2018, **140**, 7206–7212; (*c*) I. Nakase, M. Miyai, K. Noguchi, M. Tamura, Y. Yamamoto, Y. Nishimura, M. Omura, K. Hayashi, S. Futaki, S. Tokonami and T. Iida, *Nano Lett.*, 2022, **22**, 9805–9814.

12 (*a*) M. Batabyal, A. Upadhyay, R. Kadu, N. C. Birudukota, D. Chopra and S. Kumar, *Inorg. Chem.*, 2022, **23**, 8729–8745; (*b*) S. Jain, S. S. Satpute, R. K. Jha, M. S. Patel and S. Kumar, *Chem.–Eur. J.*, 2024, **30**, e202303089; (*c*) M. Batabyal, S. Jaiswal, R. K. Jha and S. Kumar, *J. Am. Chem. Soc.*, 2024, **146**(1), 57–61.

13 (*a*) S. Jana, A. Verma, R. Kadu and S. Kumar, *Chem. Sci.*, 2017, **8**, 6633–6644; (*b*) V. Rathore and S. Kumar, *Green Chem.*, 2019, **21**, 2670–2676; (*c*) R. K. Jha, A. Upadhyay, S. J. Kanika, K. A. Neena and S. Kumar, *Org. Lett.*, 2022, **24**, 7605–7610; (*d*) R. K. Jha, M. Batabyal and S. Kumar, *J. Org. Chem.*, 2023, **88**, 7401–7424; (*e*) R. K. Jha, K. Rohilla, S. Jain, D. Parganiha and S. Kumar, *Chem.–Eur. J.*, 2024, **30**, e202303537.

14 (*a*) S. Biswas, T. Dutta, D. Chopra, A. Silswal, R. Bhowal and A. L. Koner, *Chem. Sci.*, 2021, **12**, 9630–9644; (*b*) T. Dutta, S. Das, I. Gupta and A. L. Koner, *Chem. Sci.*, 2022, **13**, 12987–12995; (*c*) B. Chakraborty, S. Biswas, A. Pramanik and A. L. Koner, *ACS Appl. Mater. Interfaces*, 2022, **14**, 55957–55970; (*d*) N. Dubey, S. Dhiman and A. L. Koner, *ACS Appl. Nano Mater.*, 2023, **6**, 4078–4096.

15 Reports on the synthesis of angular phenothiazines: (*a*) C. O. Okafor, *Tetrahedron*, 1986, **42**, 2771–2775; (*b*) W. B. Kang, S. Nańya, E. Maekawa and Y. Ueno, *J. Heterocycl. Chem.*, 1988, **25**, 113–117; (*c*) E. L. Ayuk, A. N. Njokunwogbu, S. U. Ilo, G. A. Engwa, U. C. Okoro and T. O. Oni, *Am. J. Org. Chem.*, 2015, **5**, 78–81; (*d*) I. A. Ikenna, O. U. Chris and J. A. David, *Chem. Mat. Res.*, 2015, **7**, 144–146; (*e*) B. E. Ezema, C. G. Ezema, J. I. Ayogu, D. I. Ugwu and E. A. Onoabedje, *Orient. J. Chem.*, 2015, **31**, 379–385; (*f*) E. A. Onoabedje, B. E. Ezema, S. A. Egu, F. U. Eze, C. U. Ibeji, F. N. Ibeanu and U. S. Oruma, *Asian J. Chem.*, 2017, **29**, 1–3; (*g*) Q. Zhang and G. Zhang, *ChemistrySelect*, 2021, **6**, 4312–4318; Reports on cellular applications using angular phenothiazines: (*h*) C. O. Okafor, *Dyes Pigm.*, 1986, **7**, 249–287; (*i*) E. M. Odin, P. K. Onoja and J. F. Saleh, *Int. J. Phys. Sci.*, 2013, **8**, 1374–1381; (*j*) E. U. Godwin-nwakwasi, U. C. Okoro, A. O. Ijeomah, I. Agbo and M. A. Ezeokonkwo, *Asian J. Chem.*, 2017, **29**, 742–748; (*k*) E. M. Odin, S. A. Egu and K. J. Okere, *Pharm. Chem. J.*, 2020, **7**, 43–53.

16 (*a*) J. M. Bruce and P. Knowles, *J. Chem. Soc. C*, 1966, 1627–1634; (*b*) J. M. Bruce, D. Creed and J. N. Ellis, *J. Chem. Soc. C*, 1967, 1486–1490; (*c*) J. M. Bruce and K. Dawes, *J. Chem. Soc. C*, 1970, 645–648; (*d*) J. M. Bruce and D. Creed, *J. Chem. Soc. C*, 1970, 649–653; (*e*) J. M. Bruce, D. Creed and K. Dawes, *J. Chem. Soc. C*, 1971, 3749–3756; (*f*) J. M. Bruce and A.-u.-h. Chaudhry, *J. Chem. Soc., Perkin Trans. 1*, 1972, 372–379; (*g*) J. M. Bruce and A.-u.-h. Chaudhry, *J. Chem. Soc., Perkin Trans. 1*, 1974, 295–297; (*h*) F. Müh, C. Glöckner, J. Hellmich and A. Zouni, *Biochim. Biophys. Acta*, 2012, **1817**, 44–65.

17 (*a*) For ibuprofen: H. Miao, M. Guan, T. Xiong, G. Zhang and Q. Zhang, *Angew. Chem., Int. Ed.*, 2023, **62**, e2022139; (*b*) For flurbiprofen, gemfibrozil, clofibric acid, and fenbufen: A. Granados, R. K. Dhungana, M. Sharique, J. Majhi and G. A. Molander, *Org. Lett.*, 2022, **24**, 4750–4755.

18 (*a*) E. J. Corey, J. D. Bass, R. LeMahieu and R. B. Mitra, *J. Am. Chem. Soc.*, 1964, **86**, 5570–5583; (*b*) *Handbook of Synthetic Photochemistry*, ed. A. Albini and M. Fagnoni, VCH, Weinheim, 2009; (*c*) S. Poplata, A. Tröster, Y.-Q. Zou and T. Bach, *Chem. Rev.*, 2016, **116**, 9748–9815; (*d*) H. Yu, S. Dong, Q. Yao, L. Chen, D. Zhang, X. Liu and X. Feng, *Chem.–Eur. J.*, 2018, **24**, 19361–19367; (*e*) T. Lei, C. Zhou, X.-Z. Wei, B. Yang, B. Chen, C.-H. Tung and L.-Z. Wu, *Chem.–Eur. J.*, 2019, **25**, 879–884; (*f*) D. Sarkar, N. Bera and S. Ghosh, *Eur. J. Org Chem.*, 2020, 1310–1326; (*g*) D. K. Kölmel, A. S. Ratnayake, M. E. Flanagan, M. H. Tsai, C. Duan and C. Song, *Org. Lett.*, 2020, **22**, 2908–2913; (*h*) F. M. Hörmann, C. Kerzig, T. S. Chung, A. Bauer, O. S. Wenger and T. Bach, *Angew. Chem., Int. Ed.*, 2020, **59**, 9659–9668; (*i*) T. Rigotti, R. M. Ballesté and J. Alemán, *ACS Catal.*, 2020, **10**, 5335–5346.